New Phytologist

Research

Prezygotic mate selection is only partially correlated with the expression of *NaS*-like RNases and affects offspring phenotypes

Patrycja Baraniecka[1], Wibke Seibt[1], Karin Groten[1], Danny Kessler[1], Erica McGale[2], Klaus Gase[1], Ian T. Baldwin[1] and John R. Pannell[2]

[1]MPI for Chemical Ecology, Hans-Knöll-Str. 8, Jena, 07745, Germany; [2]Department of Ecology and Evolution, University of Lausanne, Lausanne, CH-1015, Switzerland

Author for correspondence:
Patrycja Baraniecka
Email: pbaraniecka@ice.mpg.de

Received: *18 December 2023*
Accepted: *21 March 2024*

New Phytologist (2024)
doi: 10.1111/nph.19741

Key words: mate selection, *Nicotiana attenuata*, postpollination ethylene burst, reproductive strategy, self-incompatibility, S-like-RNase, trade-off.

Summary

- *Nicotiana attenuata* styles preferentially select pollen from among accessions with corresponding expression patterns of *Na*S-like-RNases (SLRs), and the postpollination ethylene burst (PPEB) is an accurate predictor of seed siring success. However, the ecological consequences of mate selection, its effect on the progeny, and the role of SLRs in the control of ethylene signaling remain unknown.
- We explored the link between the magnitude of the ethylene burst and expression of the SLRs in a set of recombinant inbred lines (RILs), dissected the genetic underpinnings of mate selection through genome-wide association study (GWAS), and examined its outcome for phenotypes in the next generation.
- We found that high levels of PPEB are associated with the absence of SLR2 in most of the tested RILs. We identified candidate genes potentially involved in the control of mate selection and showed that pollination of maternal genotypes with their favored pollen donors produces offspring with longer roots. When the maternal genotypes are only able to select against nonfavored pollen donors, the selection for such positive traits is abolished.
- We conclude that plants' ability of mate choice contributes to measurable changes in progeny phenotypes and is thus likely a target of selection.

Introduction

Flowering plants have evolved a number of ways to regulate their mating systems through various reproductive barriers that involve pollen–pistil interactions, self- vs nonself-recognition and pollen preference (Pannell & Voillemot, 2017; Whitehead *et al.*, 2018). One of the best characterized examples is the rejection of self-pollen in self-incompatible (SI) species, which minimizes the deleterious effects of elevated homozygosity and inbreeding depression in progeny (Muñoz-Sanz *et al.*, 2020; Goring *et al.*, 2022). All three SI systems known to date utilize the highly polymorphic female- and male-specific S-determinants, but act via different rejection mechanisms. In the Brassicaceae and *Papaver*, the rejection of the incompatible pollen tubes of self-pollen is based on self-recognition, while the S-RNase-based system in the Solanaceae employs a nonself-recognition mechanism (Fujii *et al.*, 2016). In self-incompatible tobacco, the female S-determinant encodes pistil-specific S-RNases that inhibit the growth of incompatible pollen tubes of self-pollen by degrading their RNA via cytotoxic activity (McClure *et al.*, 1990). The pollen-specific S-determinant encodes multiple *S-locus F-box* (*SLF*) genes (Sun *et al.*, 2018) that neutralize different allelic variants of S-RNases (Kubo *et al.*, 2010). The SI-specific factors such as S-RNases, SLF proteins, HT-B and Cullin have also been shown to be involved in unilateral incompatibility between species (UI; Li & Chetelat, 2015), involving the rejection of pollen from self-compatible species by self-incompatible females, but not vice versa (Hancock *et al.*, 2003).

Polyandrous prezygotic mate selection was recently identified in *Nicotiana attenuata*, a self-compatible (SC) diploid wild tobacco species in which every cross is accepted and self-fertilization is common (Bhattacharya & Baldwin, 2012; Guo *et al.*, 2019). However, in genetically diverse natural populations with high outcrossing rates (Sime & Baldwin, 2003), certain pollen donors are consistently favored over others. The study of the molecular basis of prezygotic mate selection revealed the involvement of two *NaS-like-RNases* (*SLRs*) and six *NaSLF-like* genes that are homologues to the self-incompatibility factors in the Solanaceae. In their mixed pollination experiment with 14 nonself-pollen donors, Guo *et al.* (2019) showed that accessions of *N. attenuata* that express SLRs favor mates with a corresponding SLR expression pattern (Fig. 1a,b). Briefly, lines expressing both SLRs were found to strongly favor pollen donors with the same SLR expression pattern (Fig. 1a,b, in gray), while natural accessions and transgenic lines expressing only SLR1 strongly disfavored pollen donors that do not express SLRs (Fig. 1a,b, in pink). Natural and transgenic lines that completely lack the stylar SLR expression do not show differences in pollen preference (Fig. 1a,b, in blue; Guo *et al.*, 2019). Mate selection in *N. attenuata* occurs in the upper part of the style, and pollination with favored

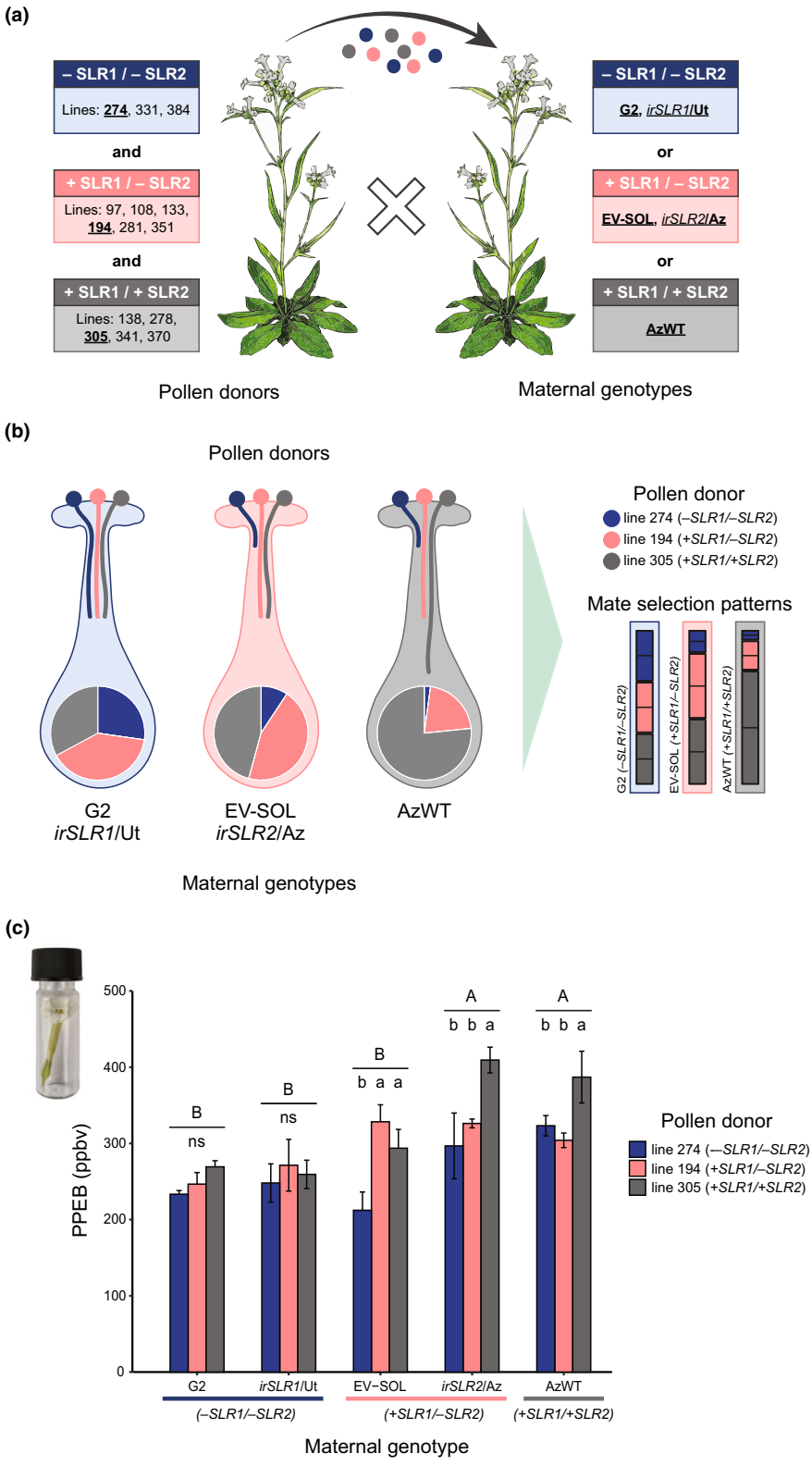

Fig. 1 The mate selection patterns in *Nicotiana attenuata* mixed pollination correlate with the expression pattern of the self-incompatibility factors S-like-RNases (SLRs) in the maternal genotypes, but the postpollination ethylene burst (PPEB) only partially corresponds to this pattern. (a, b) Schematic representation of mate selection patterns described previously (Guo *et al*., 2019). (a) Pollen donors (left) and maternal genotypes (right) can be divided into three groups depending on the expression of SLRs: lines that do not express either of the two SLRs (blue); lines that express only SLR1 (pink); and lines that express both SLRs (gray). The representative lines selected from each SLR expression group for further experiments are underlined. (b) Styles preferentially select pollen from accessions with the corresponding SLR expression pattern. Different lengths of the pollen tubes indicate mate selection processes in the styles with different SLR expression profile, while the schematic pie charts represent the percentage of seed siring success by different pollen donors shown in (a) after mixed pollination, according to Guo *et al*. (2019). The resulting mate selection patterns are summarized in the legend (right). (c) PPEB in genotypes shown in (b) after single pollination with a representative pollen donor from each SLR expression group. Data are shown as means ± SE, $n = 3$. The statistical differences were calculated using two-way ANOVA and Tukey HSD *post hoc* tests; upper-case letters indicate significant differences between maternal genotypes while lowercase letters indicate significant differences between pollen donors, ns, not significant; $P < 0.05$.

pollen results in a predictably higher postpollination ethylene burst (PPEB). Importantly, the ability of mate choice is completely lost when ethylene signaling is disrupted (Bhattacharya & Baldwin, 2012). Ethylene signaling plays a pivotal role in pollen recognition, and the variation in ethylene burst is associated with the efficiency with which pollen tubes penetrate the pistil (De Martinis *et al*., 2002). It has been shown that PPEB promotes pollen tube growth through the stylar transmitting tract (Holden *et al*., 2003; Jia *et al*., 2018) and that it can modify the cell wall structure of growing pollen tubes through the regulation of genes involved in

pectin and hemicellulose modifications (Althiab-Almasaud *et al.*, 2021).

The ecological function of prezygotic mate selection and the exact role of the SI elements in a fully self-compatible species are still not well understood. It has been suggested that the SI elements might have been repurposed during the transition from SI to SC to facilitate mate selection via a mechanism that differs from the cytotoxic activity usually associated with the classic SI model (Takayama & Isogai, 2005). Alternatively, the transition to SC could have rendered the SI system nonfunctional, resulting in gradual pseudogenization of its elements. As a consequence, the accessions expressing the SLRs might be in a transitional stage, with their fitness reduced compared to accessions that have already lost the SLR expression (Guo *et al.*, 2019). Considering that the absence of SLR expression and the disruption of ethylene signaling both lead to the loss of mate selection abilities, we examined whether variation in PPEB mirrors the mate selection patterns driven by SLR expression. Our initial results motivated a genome-wide association study (GWAS) on PPEB data from a Multiparent Advanced Generation Inter-Cross (MAGIC) population to identify novel regulatory elements involved in the mate selection processes. We hypothesized that these mechanisms may have evolved to select particular mates with traits linked to certain SLR expression patterns, and we show that they have a quantifiable effect on the phenotype of progeny and might, therefore, be targets of selection.

Materials and Methods

Plant material

Nicotiana attenuata Torrey Ex Watson (Baldwin & Morse, 1994) Utah (UtWT) and Arizona (AzWT) wild-type seeds were originally collected from a large natural population growing near Santa Clara, Utah, USA (Halitschke *et al.*, 2000), and a 20-plant population near Flagstaff, AZ, USA (Glawe *et al.*, 2003), respectively. They were inbred for 30 and 21 generations in a glasshouse (UtWT and AzWT, respectively). Furthermore, seeds of natural accession G2 were also collected in Utah, USA (Schuman *et al.*, 2009). The seeds of natural accessions used as pollen donors: lines 274, 194 and 305 were collected from different populations throughout southwestern US as described previously (Li *et al.*, 2015; Guo *et al.*, 2019) and inbred for one generation in the glasshouse. Selected recombinant inbred lines (RILs) of a 26-parent Multiparent Advanced Generation Inter-Cross (MAGIC) population were used, including one replicate of the entire population (650 lines). The population is 99% homozygous and has minimal population structure and high phenotypic and genetic diversity (Ray *et al.*, 2023). Additionally, a UtWT inbred line silenced in the expression of *NaS-like-RNase1* (*irSLR1*/UT, pSOL8SRN1, A-17-091-7), and an AzWT inbred line silenced in the expression of *NaS-like-RNase2* (*irSLR2*/AZ, pSOL8SRN2, A-17-059-6; Guo *et al.*, 2019) were used. An empty vector (EV-SOL, pSOL3NC, A-04-266-3) was used as an additional control for the transgenic lines and the analysis of the offspring, as the mate selection pattern for this specific line had been characterized previously (Bhattacharya & Baldwin, 2012; Guo *et al.*, 2019). EV-SOL was produced from the UtWT inbred line and is hence isogenic except for a single T-DNA insertion and potential uncharacterized changes that might have occurred during the transformation process (Bubner *et al.*, 2006).

Growth conditions

For the single pollination experiment and the ethylene measurements as well as for the selected MAGIC RIL lines, seeds were germinated as described previously (Krügel *et al.*, 2002) and grown in the glasshouse under long day conditions (26 ± 1°C; 16 h : 8 h, light : dark). For the seedling phenotyping experiment, seeds were germinated on square (12 cm × 12 cm) plates with GB5 medium. The plates were placed vertically in a Percival growth chamber (CLF PlantClimatics GmbH, Wertingen, Germany) for 14 d (26 ± 1°C; 16 h : 8 h, light : dark, 75% light intensity). The seeds of the MAGIC RIL lines grown for the GWAS experiment were first treated with 50× diluted liquid smoke solution (House of Herbs, Passaic, NJ, USA) and 0.1 M GA_3 for 1 h, followed by overnight incubation in the fridge in 100× diluted smoke. Subsequently, they were directly sown into 4 l pots and covered with a transparent, plastic cup for 12–16 d until the cotyledons turned to a mat green color. The cup was then removed gradually to allow further growth of the seedlings.

Single pollination experiment

The natural accessions and transgenic lines used as parental genotypes were selected on the basis of their expression of *Na*S-like-RNases: line 274, which does not express SLR1 or SLR2; line 194, which expresses only SLR1; and line 305, which expresses both SLR1 and SLR2 served as the pollen donors. AzWT served as maternal genotype known to express both SLRs, EV-SOL and *irSLR2*/Az (AzWT transgenic line silenced in the expression of SLR2) served as maternal genotypes expressing only SLR1, and natural accession G2 and the transgenic line *irSLR1*/Ut (UtWT transgenic line silenced in the expression of SLR1) served as maternal genotypes that lack the stylar expression of SLRs (Fig. 1a,b; Guo *et al.*, 2019). In the morning before the experiment (06:00 h–08:00 h), mature, open flowers and seed capsules were removed from all the plants. To prevent self-pollination, anthers were removed from the remaining, immature flowers of the maternal genotypes, as described previously (Kessler *et al.*, 2008). Single pollination was performed in the evening (18:00–20:00 h) once all the flowers had opened and the anthers of the pollen donors had matured by gently rubbing an anther over the stigma. The pollinated flowers were labeled with different colors of threads for each pollen donor tied around the pedicel. Depending on the flower availability, four to six flowers uniformly distributed around the plant, were pollinated by a single pollen donor. The matured capsules were collected *c.* 2 wk later, just before their opening, and further dried in silica gel.

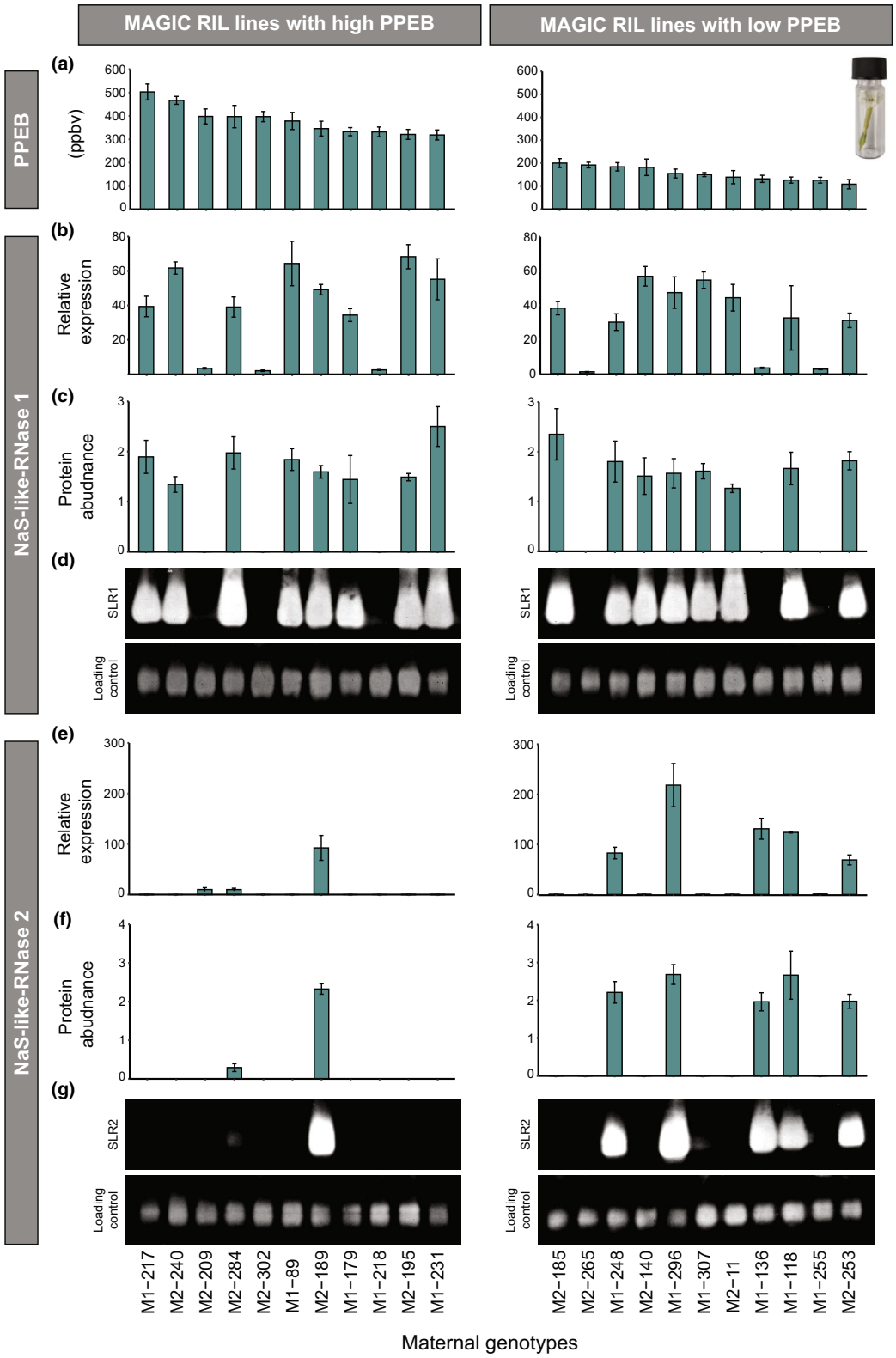

Fig. 2 A high magnitude of the postpollination ethylene burst (PPEB) correlates with the lack of expression of SLR2 in *Nicotiana attenuata*. (a) Quantification of the postpollination ethylene burst (PPEB) in recombinant inbred lines (RILs) from the 26-parent Multiparent Advanced Generation Inter-Cross (MAGIC) population with extreme phenotypes (high and low) of PPEBs when pollinated with a control, Utah wild-type accession (UtWT). Data are shown as means ± SE (n = 6). Gene expression of (b) *SLR1* and (e) *SLR2* measured in unpollinated styles relative to *N. attenuata* elongation factor 1a *NaEF1a*. Protein abundance of (c) SLR1 and (f) SLR2 quantified from the X-ray films shown in (d, g), respectively, based on mean signal intensity relative to an anti-actin loading control using Fiji software. Data are shown as means ± SE (n = 5). The brightness and contrast of the western blot results (d, g) were adjusted for imaging purposes, but not before the intensity measurement.

Ethylene measurements

To ensure that the age of flowers used for the measurements was the same across plants, all mature, open flowers and seed capsules were cut from parental genotypes either around noon (11:00 h–12:00 h) for the next-day morning measurement of the MAGIC RIL lines, or early in the morning (06:00 h–08:00 h) for measurement of the maternal genotypes the same evening (Fig. 1c). Flowers of each RIL line (Fig. 2) were hand-pollinated with UtWT pollen (n = 6), and flowers of the five maternal genotypes (Fig. 1c)

were pollinated by lines 274, 194 and 305 (n = 3; see the 'Single pollination experiment' in the Materials and Methods section). Immediately after pollination, the flowers were removed from the plant and transferred to a 4 ml glass vial. After 5 h, ethylene was measured from the headspace using a highly sensitive (0.3 ppbv detection limit) ETD-300 Ethylene Detector attached to a VC-6 Valve Control Box (Sensor Sense, Nijmegen, the Netherlands) in the sample mode, as described previously (Bhattacharya & Baldwin, 2012).

Quantitative reverse transcription polymerase chain reaction

We used quantitative reverse transcription polymerase chain reaction to investigate the accumulation of transcript abundance of the genes encoding the *SLR1* and *SLR2*. RNA was extracted from at least five unpollinated styles per replicate (n = 5) using the 'DNA, RNA, and protein purification' kit (Macherey-Nagel GmbH & Co. KG, Düren, Germany) according to the manufacturer's instructions. The RNA samples were further processed using the 'RNA Clean and Concentrator™-5' kit (Zymo Research, Irvine, CA, USA), following the manufacturer's protocol. Total RNA was quantified using NanoDrop (Thermo Scientific, Wilmington, DE, USA), and cDNA was synthesized from 500 ng of total RNA using RevertAid H Minus reverse transcriptase and oligo (dT) primer (Fermentas, Vilnius, Lithuania). Quantitative reverse transcription polymerase chain reaction was performed using a Mx3005P PCR cycler (Stratagene, San Diego, CA, USA) and a SYBR green reaction mix with added ROX dye (Eurogentec, Liège, Belgium). The primer sequences used in this study are shown in Supporting Information Table S1. *N. attenuata* elongation factor 1a (*NaEF1a*) was used as an internal control. Quantitative reverse transcription polymerase chain reaction data were normalized using the delta–delta-Ct method.

Western blot analysis

Total protein was extracted from at least five unpollinated styles per replicate (n = 5) using the RB^+ buffer (1 M Tris–HCL, pH 7.8; 5 M NaCl; 50% Glycerol; 20% Tween20, β-Me). Briefly, 80 µl of RB^+ buffer was added to the ground tissue, and the samples were centrifuged twice for 20 min in 4°C at 21 000 ***g***. The amount of total protein was quantified by a Bradford assay using Albumin Bovine (BSA; Sigma-Aldrich, Steinheim, Germany) and the Quick Start Bradford 1× Dye Reagent (Bio-Rad Laboratories). The light absorbance was measured after 10 min at 595 nm using the Infinite M2000 microplate absorbance reader (Tecan, Grödig, Austria). The samples were then denaturized at 95°C for 5 min. 15 µg of total protein in 20 µl of sample was loaded on a 12% polyacrylamide gel and run for 40 min at 60 V followed by 90–120 min at 120 V. The protein was transferred onto a PVDF membrane using the Mini *Trans*-Blot Electrophoretic Transfer Cell (Bio-Rad Laboratories) at 320 mA for 90 min. The membrane was blocked overnight in a 5% milk solution (Carl Roth GmbH + Co. KG, Karlsruhe, Germany). Subsequently, the membrane was incubated in a 1 : 5000 dilution of the SLR1 specific polyclonal antibody or a 1 : 3000 dilution of the SLR2-specific polyclonal antibody for 1 h. Both antibodies were obtained in rabbits from the synthetically synthesized immunogens based on the protein sequence of SLR1 and SLR2 (GenScript Biotech, Leiden, the Netherlands). The membranes were then washed four times for 40 min with the 1× TBST buffer followed by 1 h incubation with commercially available anti-rabbit secondary antibody (Cytvia, Marlborough, MA, USA) and a 1 h wash with 1× TBST. The protein was detected via chemiluminescence using the ECL™ Western Blotting Detection System (Cytvia, Amersham, UK), and the signal was visualized on CL-XPosure™ Film (Thermo Scientific, Waltham, MA, USA). The films were developed and fixed using the Readymatic system (Carestream Health Inc, Zaventem, Belgium). The membranes were then stripped using the 1× Restore Western Blotting Stripping Buffer (Thermo Scientific, Rockford, IL, USA), according to the manufacturer's instructions, and blocked again in 5% milk solution overnight. Subsequently, they were incubated for 2.5 h with commercially available mouse monoclonal anti-actin antibody specific for plants (Sigma-Aldrich), diluted to 1 : 500 as a loading control. The membranes were then washed, as described, and incubated with anti-mouse IgG, peroxidase-linked, species-specific secondary antibody for 1 h (Thermo Fisher Scientific, Pittsburgh, PA, USA) followed by 1 h wash with 1× TBST. The protein was then detected via chemiluminescence and the signal visualized as described.

Genome-wide association study on PPEB data

Reciprocal hand pollination was performed on 650 recombinant inbred lines (RILs) from a MAGIC population using pollen from the UtWT accession, and UtWT was pollinated with pollen from each of the 650 RIL lines (n = 1). The PPEB was measured, as described (see 'Ethylene measurement' in the Materials and Methods section). These crosses resulted in two different datasets (Fig. S1). The initial data was examined for potential variation due to the time of pollination or differences in environmental conditions. Lines that showed inconsistent values when measured multiple times were removed from further analyses. GWAS was conducted on 629 datapoints in each dataset using the Genomic Association and Prediction Integrated Tool (GAPIT v.3) package in the R interface (Wang & Zhang, 2021). Generalized Linear Models (GLM) were used for the association analysis. Significance of associations was inferred on the basis of a logarithm of the odds (LOD) threshold of 1e−05 (Fig. S2).

Seed count and size measurement

The seeds obtained after the single pollination experiment were first removed from the dried capsule, cleaned from any remaining plant tissue, and weighed. The seeds were then scattered on a square plate, and the plate was scanned using a modified regular office scanner. The pictures were analyzed using FIJI software (v.2.3.0/1.53q) and the particle analysis tool. Seed number and average seed size data were collected and are presented as an average per capsule (Fig. 3).

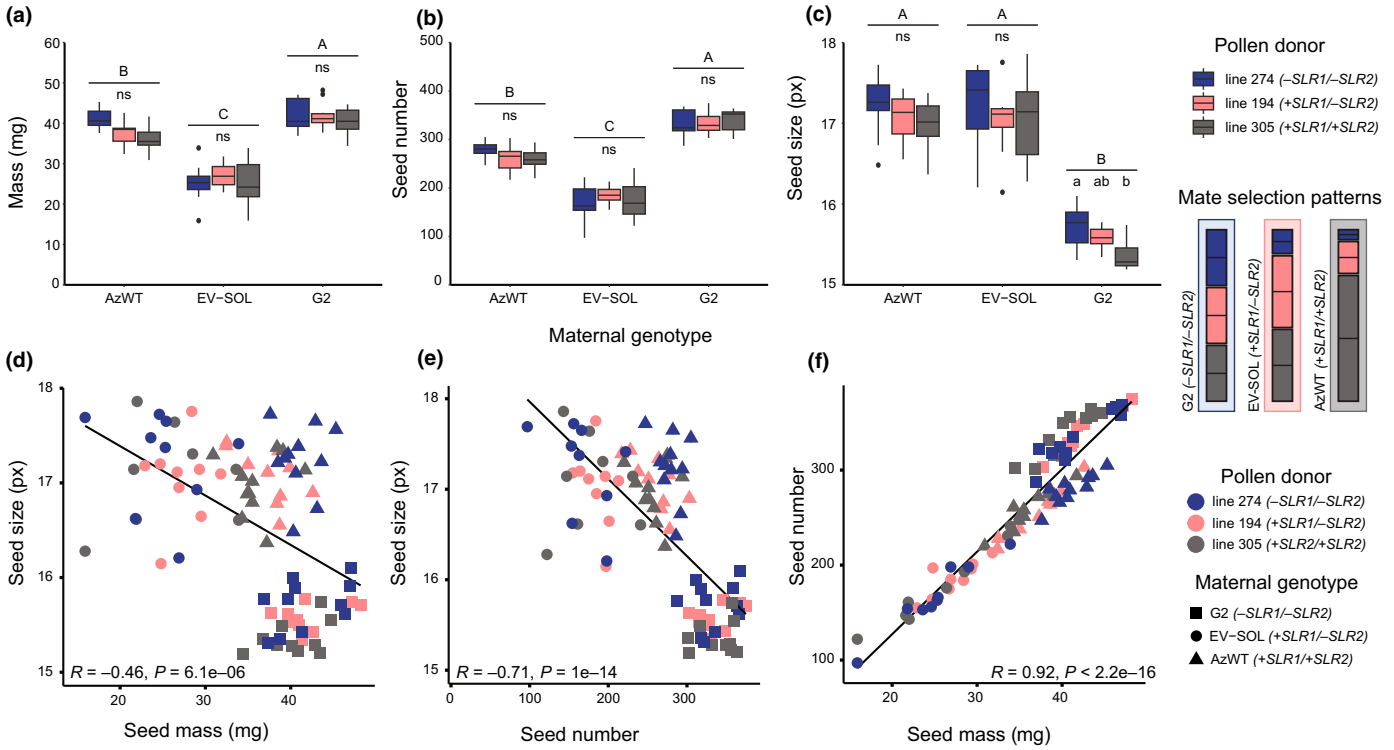

Fig. 3 The trade-off between seed size, seed mass and number in *Nicotiana attenuata* depends on maternal genotype. (a) The seed mass, (b) seed number, and (c) average seed size were calculated per capsule produced by different maternal genotypes after single hand pollination with a favored, nonfavored or neutral pollen donor. Pollen preference and mate selection patterns of different maternal genotypes are summarized in the corresponding legend (right). Data are shown as means of up to 10 capsules collected from two different plants per maternal genotype obtained after the single pollination experiment ± SE (whiskers) Mean value is indicated as a horizontal line in each box while the black circles indicate outliers. Mixed-effect models were applied where required, otherwise two-way ANOVA and a TukeyHSD *post hoc* test were used. Upper-case letters (above the line) indicate statistical differences dependent on the maternal genotype, lowercase letters (below the line) indicate statistical differences dependent on the pollen donor, ns, not significant; $P < 0.05$. (d–f) Spearman's correlation between seed size and seed mass (d), seed size and seed number (e) and seed number and (f) seed mass. The respective correlation coefficients (R) and P-values (P) are displayed on each graph.

Seedling phenotyping

Ten seeds from three capsules per cross obtained from the single pollination experiment were grown vertically for 14 d, as described (see 'Growth conditions' in the Materials and Methods section). To determine the germination time (Fig. 4), all plates were scanned daily from 3 d after sowing (DAS) using the modified regular office scanner. Once all seeds had germinated, the plates were scanned every second day from the top and bottom. The root and shoot of each seedling were collected destructively 14 DAS for biomass estimation. Data for root length, root area, hypocotyl length and rosette size were obtained from the pictures using the FIJI software (v.2.3.0/1.53q) at six different time points (Fig. 5). A representative picture of seedlings from each cross was taken using a regular mobile phone camera (Fig. S3).

Statistical analyses

All data were analyzed using R statistical Software v.4.2.1 (R Core Team, 2020) in RSTUDIO v.2022.07.1 + 554 (R Studio Team, 2020). The datasets regarding seed attributes (Fig. 3) and early seedling establishment (Fig. 5) were first tested for the effect of the individual using ANCOVA, intraclass correlation and bootstrapping. Whenever the effect of the individual was significant, the data were fit to a linear mixed-effect model (using the NLME package) to account for the influence of the nested structure of the data per individual and checked for homoscedasticity and normality through a graphical analysis of residuals (Zuur *et al.*, 2009). Otherwise, two-way ANOVAs were applied (using the EMMEANS package; Lenth *et al.*, 2019). Multiple comparisons were extracted with a Sidak (for the mixed-effect models) or TukeyHSD (for the ANOVAs) *post hoc* test. The correlations shown in Fig. 3; Table S2 were extracted using the Spearman's rank correlation coefficient. The analysis of the germination rate (Fig. 4) was performed using the *coxph()* function in the R package *survival* to calculate the Cox proportional hazards (Therneau, 2022).

Results

The magnitude of PPEB only partially corresponds with the expression of SLRs

We investigated whether pollination with favored and nonfavored pollen results in predictable changes in the magnitude of PPEB and whether this variation is dependent on the SLR

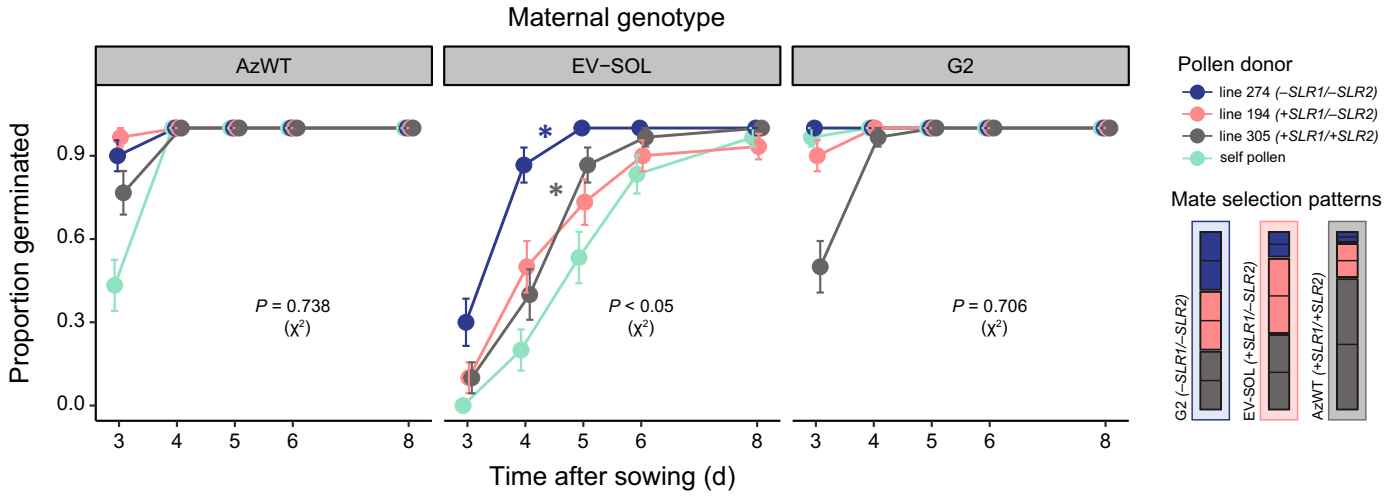

Fig. 4 In *Nicotiana attenuata* the germination time depends on maternal genotype and the pollen donors. Germination rate (proportion germinated ± SE, $n = 30$) of seeds produced by three maternal genotypes after single hand pollination with a favored, nonfavored or neutral pollen donor when compared to the germination rate of seeds produced after self-pollination based on Cox proportional hazards test. Pollen preference and mate selection patterns of different maternal genotypes are summarized in the corresponding legend (right). Self-pollen is always preferred over any other pollen donor. The overall effect of the pollen donor is indicated for each maternal genotype (χ^2). The asterisks indicate significant differences in the germination for the particular pollen donors when compared to self-pollen, $P < 0.05$.

expression in the parental genotypes. We measured the ethylene emission after hand pollination of different maternal accessions with pollen donors selected from each SLR expression group, as described in the 'Single pollination experiment' in the Materials and Methods section. Natural accession G2 and the transgenic line *irSLR1*/Ut have both lost the ability of mate selection due to the lack of the stylar expression of SLR1 and SLR2 (Fig. 1a,b). As expected, no significant differences in PPEB were observed after pollination of those maternal genotypes with the selected pollen donors (Fig. 1c). Pollination of EV-SOL (SLR1 expression) with line 274 (no SLR expression) resulted in significantly lower PPEB compared to the other two pollen donors. As EV-SOL has been shown to select strongly against the accessions with no SLR expression (Guo *et al.*, 2019), this PPEB phenotype corresponds to the mate selection pattern observed for this genotype. Pollination of the transgenic line silenced in the expression of SLR2 (*irSLR2*/Az) with pollen donor 274 resulted in a PPEB comparable to the one observed after pollination of this line with pollen donor 194 that expresses only SLR1. However, it was significantly higher after pollination with line 305 expressing both SLRs, a phenotype identical with the one observed for AzWT (Fig. 1c) that has been shown to select strongly for the pollen donors with similar SLR expression pattern (Guo *et al.*, 2019). As *irSLR2*/Az shows a PPEB phenotype similar to that of AzWT despite expressing only SLR1, like *EV-SOL*, we conclude that the control of PPEB only partially correlates with the expression of SLRs and is more complex than initially suspected. The fact that both *irSLR2*/Az and AzWT produced, on average, more ethylene than the other three maternal genotypes, despite having different SLR expression profiles, indicates that additional elements must be involved in the regulation of PPEB.

High levels of PPEB correlate with the lack of SLR2 expression

To further investigate the association between the magnitude of the PPEB and the transcript and protein abundance of the two SLRs, we quantified the PPEB in 650 recombinant inbred lines (RILs) from the MAGIC population after hand pollination with the pollen from Utah WT accession (Fig. S1). Subsequently, we selected a subset of individuals with extreme phenotypes for further testing. After reconfirming the magnitude of PPEB in these lines (Fig. 2a), we measured the stylar expression and protein abundance of both SLR1 (Fig. 2b–d) and SLR2 (Fig. 2f,g). SLR1 expression and the protein were detected in nine lines with the low PPEB and nine lines with the high PPEB. However, gene expression levels and protein abundance of SLR2 were detected in five lines with low PPEB and only one high PPEB line. We computed the Spearman's rank correlation coefficient to assess the relationship between PPEB and the SLRs (Table S2). There was no significant correlation for SLR1, but we observed a significant negative correlation between PPEB and the expression and protein abundance for SLR2 ($R = -0.38$, $R = -0.38$, respectively, $P < 0.05$). As not all of the tested lines followed this pattern, these findings further support the involvement of additional regulatory mechanisms in the control of mate selection.

GWAS identifies a major peak associated with variation in PPEB

The analysis of the association between SLR expression patterns and the PPEB in different genotypes pointed to the existence of additional regulatory elements involved in the control of mate selection. To explore the genetic architecture underlying this

process and to identify novel genes involved in its regulation, we conducted a GWAS on PPEB data obtained from the MAGIC population. The quantification of the PPEB after reciprocal single hand pollination of nearly 650 RIL lines of the MAGIC population resulted in two distinct datasets (Fig. S1): one with varied maternal genotypes and standardized pollen donor that were used to impute style-expressed genes and to elucidate the role of the maternal genotype in the mate selection processes; and one in which a standardized maternal genotype and varied pollen donors were used to impute pollen-related genes and explore signals derived from different pollen donors. We found no significant association from the analysis of the dataset with the standardized maternal genotype, whereas the GWAS of the dataset with varied maternal genotypes resulted in the identification of nine significant associations located on chromosome 9 and one association located on chromosome 4 (Fig. S2; Table S3). The phenotypic variance explained by the individual significant SNPs was c. 10%. Among the nine significant SNPs identified on chromosome 9, eight were part of a clearly identified peak of associations covering *c.* 14.5 Mbp on chromosome 9 (Fig. S2a). Therefore, in our search for the candidate genes, we included additional markers that were part of this peak, though slightly below the significance threshold (Table S3). A large number of genes were identified, assuming a linkage disequilibrium (LD) decay distance of 2.5 Mbp on either side of each significant marker. The list of candidates was narrowed down to the genes specifically expressed in the female reproductive organs based on the *N. attenuata* eFP browser (Brockmöller *et al.*, 2017). Finally, seven candidates were selected based on functional annotations and the current state of the literature, including an ethylene-responsive transcription factor, two putative leucine-rich receptor-like (LLR) protein kinases, an *N. attenuata* homolog to an early nodulin-like proteins previously identified in *A. thaliana*, and a cluster of three genes annotated as regulators of nonsense transcripts 1 (Table S4). We propose that these genes are likely to be involved in the regulation of mate selection in *N. attenuata* and should be studied in more detail.

The strength of the trade-off between offspring size and number is controlled by the maternal genotype

To investigate whether the prezygotic mate selection observed in the *N. attenuata* accessions affects the performance of the progeny, we pollinated the three previously selected maternal genotypes with the pollen donor representatives of the three SLR expression groups, and examined different seed attributes of the offspring (Fig. 3). No significant differences associated with the pollen donor were observed for seed mass and seed number. Natural accession G2 was the only maternal genotype that showed significant differences in the average seed size as a function of the pollen donor, with the largest seeds produced in the cross with line 274 and the smallest seeds produced in the cross with line 305 (Fig. 3c). Among the three maternal genotypes, EV-SOL generally showed the lowest seed mass and seed number, while G2 showed the highest (Fig. 3a,b). The strong positive correlation between those two traits was confirmed by a Spearman's rank correlation ($R = 0.92$, $P < 2.2e{-}16$; Fig. 3f). Average seed size correlated negatively with seed mass ($R = -0.46$, $P = 6.1e{-}06$; Fig. 3d) and seed number ($R = -0.71$, $P = 1e{-}14$; Fig. 3e), indicating a trade-off between offspring size and number. Indeed, the low seed count for EV-SOL resulted in larger seeds, while the high seed count in G2 resulted in the smallest seeds among the three genotypes tested. Even though AzWT produced significantly more seeds than EV-SOL, they were of a similar size (Fig. 3b,c). Together, these results illustrate that in *N. attenuata* the offspring size vs number trade-off is mainly controlled by the maternal genotype, and the function of the pollen donor is apparent only in the nonselecting line (G2).

Mate selection mechanisms affect the germination time of the progeny

To further investigate the effect of mate choice on the offspring, we examined the germination rate of the seeds obtained from the different crosses. The fastest germinating seeds were produced by natural accession G2 (Fig. 4). Within three DAS, G2 showed 100% germination in the cross with line 274, 97% when self-pollinated, and 90% when crossed with line 194. Pollination of G2 with line 305 resulted in a 11% decrease in the germination rate compared to the self-pollination, but the overall effect of the pollen donor was not significant. The germination rate of seeds produced by AzWT increased by 13% after the pollination with line 194, 11% after the pollination with line 274 and nearly 8% after the pollination with line 305 when compared to the seeds produced after the self-pollination, but the overall effect of pollen donor was not significant. By contrast, the seeds produced by EV-SOL germinated much more slowly. This genotype produced the best-performing offspring after pollination with the nonfavored line 274, which resulted in a 78% increase in the germination rate when compared to self-pollinated seeds ($P < 0.001$). Additionally, the germination rate of the EV-SOL seeds increased 34% after pollination with line 305 ($P = 0.028$) and 22% with line 194 ($P = 0.16$). These results demonstrate that pollination with nonself-pollen has an overall positive effect on the seed germination rate for most of the tested lines compared to self-pollination, and that the pollen donor affects the germination time.

Seedling establishment and early growth dynamics depend on both parental genotypes

To evaluate if variation in seed size and number as well as in the germination time affects seedling establishment, we measured the shoot- and root-related traits of the seedlings from the different crosses 14 DAS (Figs 5, S3). Additionally, we monitored the growth of the seedlings every two days to provide a detailed description of the early growth dynamics (Figs S4, S5). The fastest-growing offspring in this experiment was obtained from a cross of EV-SOL and line 274. The seedlings obtained from this cross exceeded in all the traits measured in this experiment except for hypocotyl length. They showed the longest tap root and the highest number of lateral roots (Fig. S4c), resulting in the highest

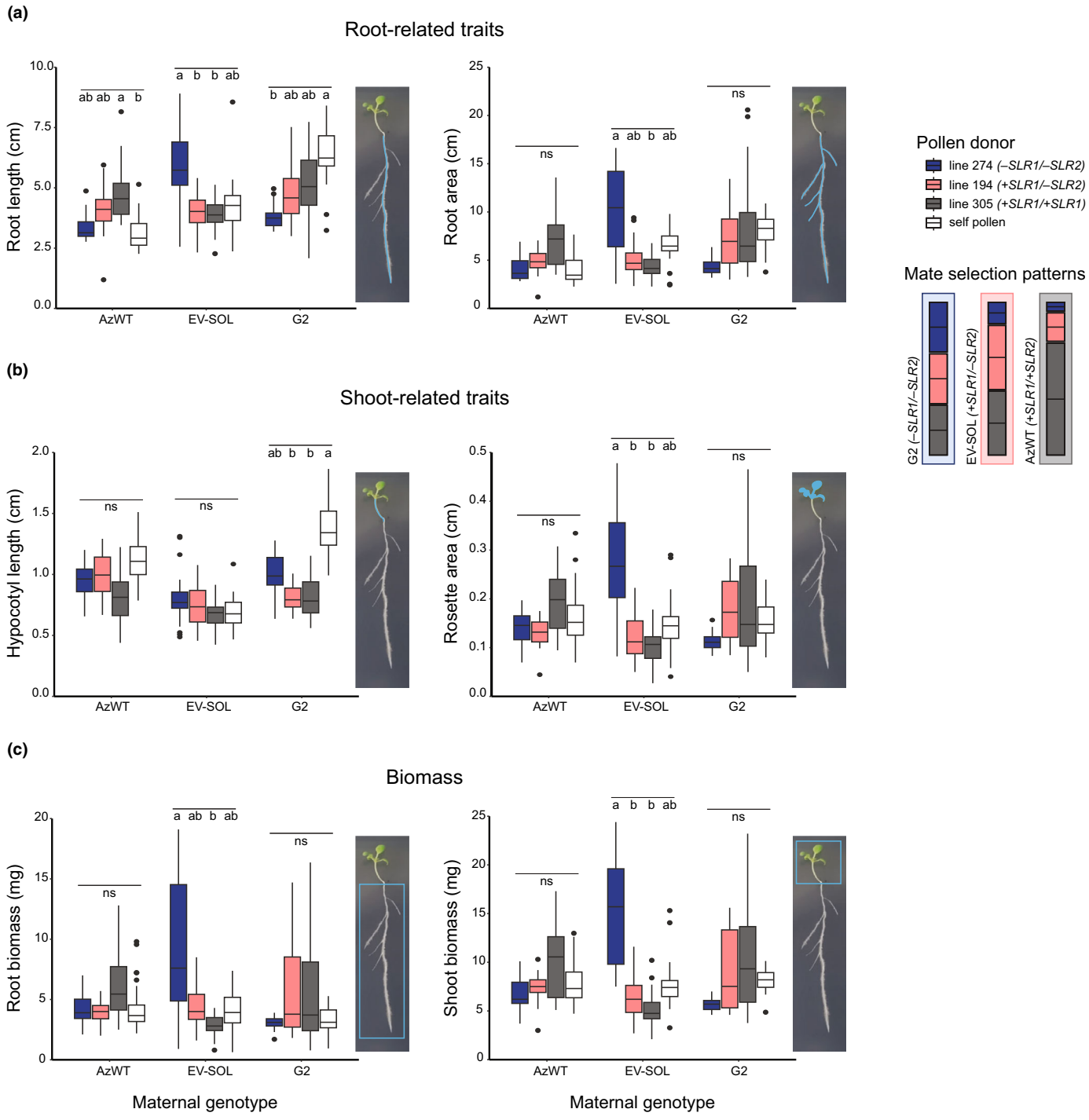

Fig. 5 Early establishment of *Nicotiana attenuata* seedlings depends on maternal genotype and pollen donor. The phenotypic traits of the offspring obtained from the hand pollination of different maternal genotypes with favored, nonfavored, neutral or self-pollen were quantified 14 d after sowing (DAS). Pollen preference and mate selection patterns of different maternal genotypes are summarized in the corresponding legend (right). Self-pollen was always preferred over any other pollen donor. (a) Root-related traits (the length of the tap root and root area shown as the sum of lengths of tap root and secondary roots), and (b) shoot-related traits (hypocotyl length and rosette area) were measured from scans of the seedlings using ImageJ. (c) Root and shoot biomass were measured following destructive sampling at the end of the experiment. Data are shown as means of up to 30 seedlings per cross ± SE (whiskers, 10 randomly selected seeds from the three different capsules obtained from singSensorle pollination experiment; related data in Figs 3 and 4). Mean value is indicated as a horizontal line in each box while the black circles indicate outliers. Statistical differences were calculated using mixed-effect models with a Sidak *post hoc* test to extract multiple comparisons; lowercase letters (below the line) indicate statistical differences dependent on the pollen donor, ns, not significant; $P < 0.05$.

root biomass. These individuals entered the logarithmic phase of growth faster than all the other seedlings (Fig. S4) and produced the largest rosettes and the highest shoot biomass. On the other hand, the seedlings obtained from the cross between AzWT and its favored pollen donor (line 305) were consistently slightly larger than those from the other pollen donors (Figs 5, S3–S5). However, since only the results observed for the root length were statistically significant, this tendency would have to be further verified. The cross of G2 with line 194 produced fewer, but longer, lateral roots, whereas the cross with line 305 resulted in a large number of short lateral roots, demonstrating that differences in early root architecture depend on the pollen donor (Figs 5, S4c). G2 seedlings were also characterized by very long hypocotyls, especially after self-pollination (Fig. 5b). Taken together, these results indicate that the mate selection mechanisms and different reproductive strategies observed in *N. attenuata* result in differences in offspring growth phenotypes that are already visible at the early stages of seedling establishment.

Discussion

Disruption of ethylene signaling in ethylene-deficient mutants and the lack or loss of the expression of the *Na*S-like RNases (SLRs) have both been shown to result in the loss of mate selection abilities of various *Nicotiana attenuata* genotypes (Bhattacharya & Baldwin, 2012; Guo *et al.*, 2019), but have not previously been investigated for potential links in their function. Therefore, we first explored whether the variation in the SLR expression profiles of different genotypes is linked to ethylene signaling. We found that the PPEB is only partially correlated with the SLR expression and that some of the observed variation depends on the genetic background of the maternal genotype rather than the SLR expression pattern (Fig. 1c). Moreover, our results illustrate that a high level of PPEB after pollination with a standard pollen donor is associated with the lack of stylar expression of SLR2 (Fig. 2; Table S2). This conclusion is also supported by the higher PPEB levels observed after pollination of UtWT accession, which expresses only SLR1 with pollen from different MAGIC lines compared to the dataset where MAGIC lines, many of which do express SLR2, were pollinated with the pollen from UtWT (Fig. S1). The lack of any specific correlation between the magnitude of PPEB and the expression of SLR1 points to a difference in the regulation of the two SLRs and possibly in their function in facilitating the prezygotic mate selection. It has been shown that variation in the SLR protein abundance among natural *N. attenuata* accessions is correlated with DNA methylation (Guo *et al.*, 2019). Additionally, a recent study suggested that, in the absence of a sufficient amount of ethylene, the growth of the pollen tube might be blocked through a mechanism involving the ethylene receptors (ETRs), leading to modification of pollen tube cell walls and Ca^{2+} loading (Althiab-Almasaud *et al.*, 2021). A calcium-dependent protein kinase that phosphorylates S-RNase (Nak-1) has been identified in *Nicotiana alata*, but its specific function in SI is not clear (Kunz *et al.*, 1996). Differential phosphorylation/dephosphorylation of the two SLRs, in addition to variation in the SLR protein abundance in natural accessions, could explain the differences observed in our study and should be investigated further.

We hypothesized that the observed mate choice mechanisms could be targets of selection, potentially allowing maternal genotypes to choose mates with beneficial traits, which would ultimately lead to the production of superior progeny. To address this question, we examined the performance of the offspring obtained after pollination with favored and nonfavored pollen donors. The analysis of the differences in the seed size and seed number per capsule among the different crosses revealed the existence of a trade-off between offspring size and number (Fig. 3). Such offspring size vs number trade-offs are common among the plant and animal kingdoms (Fox & Czesak, 2000; Gnan *et al.*, 2014; Dani & Kodandaramaiah, 2017), yet our results show that their level may vary between different genotypes. We observed that the pollination with the preferred pollen donor results in production of progeny with larger roots compared to the self-pollen in the *N. attenuata* accessions that are able to choose their preferred pollen donors (e.g. AzWT in the cross with line 305). This tendency, even though not significant for other traits, was consistently observed across experiments (Fig. 5). By contrast, lines that do not have or cannot choose their favored pollen donors, but are able to discriminate against the nonfavored ones (such as the maternal genotypes that express only SLR1), produced the largest and fastest-growing progeny overall after the cross with the nonfavored pollen (Figs 5, S3). Guo *et al.* (2019) have shown that pollen donors that do not express any SLRs are disfavored by the maternal genotypes that express the SLRs, regardless of the exact pattern (Fig. 1b). We speculate that the rejection of pollen tubes from these donors could be correlated with the expression of SLR1 specifically, further supporting our hypothesis that the two SLRs differ in their function in mate selection, for example SLR1 could inhibit the growth of pollen tubes while SLR2 could facilitate it. To test this hypothesis, pollen tube growth rates would have to be measured for different crosses, including in genotypes that express only SLR2. Alternatively, it is possible that the loss of SLRs was accompanied by the loss of other elements linked to the S-locus that are necessary for mate selection. As a consequence, the pollen tubes from accessions with no SLR expression would be inhibited by the maternal genotypes that express SLRs due to the lack of necessary interacting proteins delivered by the pollen, regardless of the potential benefit of producing superior offspring. Such disparity would render these maternal genotypes incapable of taking advantage of the high-quality mate, reducing the overall performance of its offspring and consequently, the fitness of the maternal line itself. The exact molecular mechanism of mate selection is still not known, but an obvious first step to test our hypothesis would be to investigate the expression of pollen-specific S-determinants as well as genes homologous to non-S-locus modifiers and their interaction with the two SLRs in the parental genotypes. As the reproductive success of an individual is measured not only by the number of their offspring, but also by their offspring's ability to produce further

offspring of their own, more research is needed to determine whether mate selection is adaptive.

The finding that the maternal genotype expressing only SLR1 failed to yield a greater number of larger and faster growing progeny when crossed with line 274 points to the reduced fitness of this genotype compared to the other two accessions. This observation supports the hypothesis that the SI elements are being pseudogenized after the SI-SC transition of *N. attenuata*, which might affect the performance of genotypes that still express at least one of the SLRs (Guo *et al.*, 2019). This hypothesis is also supported by results observed for the offspring of the nonselecting maternal line, G2 (Fig. 5), for which the offspring size vs number trade-off was much more pronounced, but its direction changed compared to the other two maternal genotypes (Fig. 3). This nonselecting maternal genotype produced a large number of small seeds with different genetic qualities. Its offspring had longer hypocotyls and larger root systems which might contribute to improved efficiency in transitioning from the heterotrophic to autotrophic lifestyle (Zacchello *et al.*, 2020) and competing for limiting resources (Mašková & Herben, 2018). This kind of phenotypic plasticity at the early stages of development would be beneficial in the context of the natural history of *N. attenuata*. The fire-dependent seed germination in this species results in long dormancy periods followed by germination and growth in genetically diverse populations (Bahulikar *et al.*, 2004). The production of many genetically diverse offspring might reflect an adaptive bet-hedging strategy, with implications for the survival of long-lived seed banks and accounting for different growth conditions after germination (Anderson *et al.*, 2023). In fact, G2 was the only maternal genotype that showed significant differences in the seed size dependent on the pollen donor, suggesting differential maternal investment in the genetically variable offspring and possibly a higher level of parent offspring conflict (Smith & Fretwell, 1974; Raunsgard *et al.*, 2018). Although it has been shown previously that the variation in seed size can affect the performance of the progeny in many species (Van Daele *et al.*, 2012; Zacchello *et al.*, 2020; Tumpa *et al.*, 2021), detailed analyses of the *N. attenuata* maternal and zygotic genetic controls on seed size and number as well as their effect on the seedbank survival and germination are required to understand the consequences of this phenotype.

Among the significant associations obtained from the pollination of different maternal genotypes with a standardized pollen donor, we identified seven potential candidates (Table S4). The gene encoding the ethylene-responsive transcription factor (*ERF061*, Niat3g_65650) is particularly interesting because of its strong expression in the style and stigma, whereas an *A. thaliana* homolog of this gene is expressed in the papillae cells and siliques. No functional analysis of this gene has been reported to date, but its highly specific expression profile indicates its potential involvement in the early stages of pollen–pistil interaction, which is where prezygotic mate selection occurs (Bhattacharya & Baldwin, 2012). Similarly, LRR protein kinases have been recently shown to be involved in early stages of pollen recognition and pollen–pistil interactions in *A. thaliana* (Lee & Goring, 2021). The involvement of receptor kinases in the later stages of the reproduction, such as pollen tube guidance to the ovule, or its reception, have been already described in great detail (Bordeleau *et al.*, 2022), but the research has mainly focused on the model system *A. thaliana*. Further characterization of the LRR protein kinases identified in our analysis (Niat3g_66018 and Niat3g_65722) could provide novel insight into the function of these proteins. By contrast, the gene annotated as the early nodulin-like protein 3 (*ENOD3*, Niat3g_65615) is expressed specifically in ovaries and flower buds, suggesting that it may act at later stages of male–female communication. Several female-specific early nodulin-like proteins have been shown to be involved in pollen tube entrance into the ovule, growth arrest and burst in *A. thaliana* (Hou *et al.*, 2016). We also identified a cluster of three genes annotated as regulators of nonsense transcript 1 (Niat3g_65293, Niat3g_65295 and Niat3g_65296) that share high homology with UPF1, an RNA helicase involved in the nonsense mutation mediated RNA decay (NMD). The NMD factors such as UPF1 and SMG7 are involved in the regulation of a number of physiological processes in plants, including ethylene signaling, meiosis, seed set and seed size control (Yoine *et al.*, 2006; Raxwal *et al.*, 2020). Additionally, there is growing evidence for a wide range of noncanonical functions of these proteins (Raxwal & Riha, 2023). Besides the potential role of NMD in supporting the degradation of RNA of the incompatible pollen, it could also fine-tune the function of other mate selection genes or act via ethylene signaling. Further work on the genes identified in this study could lead to a better understanding of the noncanonical functions of NMD factors and plant sexual reproduction.

It is clear from our results that variation in PPEB does not account for all the differences in the SLR expression profiles between the tested genotypes. The poor correlation of SLR expression with the mate choice emphasizes the need to look beyond the SI for the underlying mechanisms. Our results also demonstrate that a plant's ability to influence which pollen donor sires its progeny has implications for progeny growth and is thus likely a target of natural selection. More research is needed to fully understand the evolutionary and ecological consequences of mate selection. Functional analysis of the genes identified here will likely provide tools both for manipulating these processes to shed new light on the underlying mechanism as well as for experiments to test eco-evolutionary hypotheses.

Acknowledgements

We thank Prof. Sarah E. O'Connor for supporting the project, Evelyn Claußen, Mohammed Abdulazeez and Melanie Smith for technical support, Dr Grit Kunert for statistical advice, Dr Rayko Halitschke for help with ethylene measurements and scientific support, the glasshouse team for the plant cultivation and the members of the department for their help with germination and harvesting of the MAGIC population. This work was supported by the Max Planck Society and the Collaborative Research Centre 'Chemical Mediators in Complex Biosystems-ChemBioSys' (SFB 1127) to ITB. Open Access funding enabled and organized by Projekt DEAL.

Competing interests

None declared.

Author contributions

PB, ITB and JRP provided the intellectual framework for the study, PB and WS designed and performed the experiments with the help of EM, and PB and EM analyzed the data. The original manuscript was prepared by PB with the help of Karin Groten, DK, WS and Klaus Gase. All authors contributed intellectually to the study as well as reviewed and agreed to this manuscript.

ORCID

Ian T. Baldwin https://orcid.org/0000-0001-5371-2974
Patrycja Baraniecka https://orcid.org/0009-0001-9684-6021
Klaus Gase https://orcid.org/0000-0002-8028-5645
Karin Groten https://orcid.org/0000-0003-0177-8810
Danny Kessler https://orcid.org/0000-0003-0410-116X
Erica McGale https://orcid.org/0000-0002-5996-4213
John R. Pannell https://orcid.org/0000-0002-0098-7074

Data availability

All data supporting the findings of this work are available in the Edmond Open Research Data Repository, doi: 10.17617/3.B0T72Y.

References

Althiab-Almasaud R, Chen Y, Maza E, Djari A, Frasse P, Mollet JC, Mazars C, Jamet E, Chervin C. 2021. Ethylene signaling modulates tomato pollen tube growth through modifications of cell wall remodeling and calcium gradient. *The Plant Journal* **107**: 893–908.

Anderson B, Pannell J, Billiard S, Burgarella C, de Boer H, Dufay M, Helmstetter AJ, Méndez M, Otto SP, Roze D *et al.* 2023. Opposing effects of plant traits on diversification. *iScience* **26**: 106362.

Bahulikar RA, Stanculescu D, Preston CA, Baldwin IT. 2004. ISSR and AFLP analysis of the temporal and spatial population structure of the post-fire annual, *Nicotiana attenuata*, in SW Utah. *BMC Ecology* **4**: 12.

Baldwin IT, Morse L. 1994. Up in smoke 2. Germination of *Nicotiana attenuata* in response to smoke-derived cues and nutrients in burned and unburned soils. *Journal of Chemical Ecology* **20**: 2373–2391.

Bhattacharya S, Baldwin IT. 2012. The post-pollination ethylene burst and the continuation of floral advertisement are harbingers of non-random mate selection in *Nicotiana attenuata*. *The Plant Journal* **71**: 587–601.

Bordeleau SJ, Canales Sanchez LE, Goring DR. 2022. Finding new *Arabidopsis* receptor kinases that regulate compatible pollen-pistil interactions. *Frontiers in Plant Science* **13**: 1022684.

Brockmöller T, Ling Z, Li D, Gaquerel E, Baldwin IT, Xu S. 2017. *Nicotiana attenuata* Data Hub (NaDH): an integrative platform for exploring genomic, transcriptomic and metabolomic data in wild tobacco. *BMC Genomics* **18**: 79.

Bubner B, Gase K, Berger B, Link D, Baldwin IT. 2006. Occurrence of tetraploidy in *Nicotiana attenuata* plants after *Agrobacterium*-mediated transformation is genotype specific but independent of polysomaty of explant tissue. *Plant Cell Reports* **25**: 668–675.

Dani KGS, Kodandaramaiah U. 2017. Plant and animal reproductive strategies: lessons from offspring size and number tradeoffs. *Frontiers in Ecology and Evolution* **5**: 38.

De Martinis D, Cotti G, Hekker ST, Harren FJM, Mariani C. 2002. Ethylene response to pollen tube growth in *Nicotiana tabacum* flowers. *Planta* **214**: 806–812.

Fox CW, Czesak ME. 2000. Evolutionary ecology of progeny size in arthropods. *Annual Review of Entomology* **45**: 341–369.

Fujii S, Kubo K, Takayama S. 2016. Non-self- and self-recognition models in plant self-incompatibility. *Nature Plants* **2**: 16130.

Glawe GA, Zavala JA, Kessler A, Van Dam NM, Baldwin IT. 2003. Ecological costs and benefits correlated with trypsin protease inhibitor production in *Nicotiana attenuata*. *Ecology* **84**: 79–90.

Gnan S, Priest A, Kover PX. 2014. The genetic basis of natural variation in seed size and seed number and their tradeoff using *Arabidopsis thaliana* MAGIC lines. *Genetics* **198**: 1751–1758.

Goring D, Cruz-Garcia F, Franklin-Tong V. 2022. Self-incompatibility. *Encyclopedia of Life Sciences* **2**: 1–12.

Guo H, Halitschke R, Wielsch N, Gase K, Baldwin IT. 2019. Mate selection in self-compatible wild tobacco results from coordinated variation in homologous self-incompatibility genes. *Current Biology* **29**: 2020–2030.

Halitschke R, Kessler A, Kahl J, Lorenz A, Baldwin IT. 2000. Ecophysiological comparison of direct and indirect defenses in *Nicotiana attenuata*. *Oecologia* **124**: 408–417.

Hancock CN, Kondo K, Beecher B, McClure B. 2003. The S-locus and unilateral incompatibility. *Philosophical Transactions of the Royal Society of London. Series B, Biological Sciences* **358**: 1133–1140.

Holden MJ, Marty JA, Singh-Cundy A. 2003. Pollination-induced ethylene promotes the early phase of pollen tube growth in *Petunia inflata*. *Journal of Plant Physiology* **160**: 261–269.

Hou Y, Guo X, Cyprys P, Zhang Y, Bleckmann A, Cai L, Huang Q, Luo Y, Gu H, Dresselhaus T *et al.* 2016. Maternal ENODLs are required for pollen tube reception in *Arabidopsis*. *Current Biology* **26**: 2343–2350.

Jia HL, Yang J, Liesche J, Liu X, Hu YF, Si WT, Guo JK, Li JS. 2018. Ethylene promotes pollen tube growth by affecting actin filament organization via the cGMP-dependent pathway in *Arabidopsis thaliana*. *Protoplasma* **255**: 273–284.

Kessler D, Gase K, Baldwin IT. 2008. Field experiments with transformed plants reveal the sense of floral scents. *Science* **321**: 1200–1202.

Krügel T, Lim M, Gase K, Halitschke R, Baldwin IT. 2002. *Agrobacterium*-mediated transformation of *Nicotiana attenuata*, a model ecological expression system. *Chemoecology* **12**: 177–183.

Kubo K, Entani T, Takara A, Wang N, Fields AM, Hua Z, Toyoda M, Kawashima S, Ando T, Isogai A *et al.* 2010. Collaborative non-self recognition system in S-RNase-based self-incompatibility. *Science* **330**: 796–799.

Kunz C, Chang A, Faure JD, Clarke AE, Polya GM, Anderson MA. 1996. Phosphorylation of style S-RNases by Ca^{2+}−dependent protein kinases from pollen tubes. *Sexual Plant Reproduction* **9**: 25–34.

Lee HK, Goring DR. 2021. Two subgroups of receptor-like kinases promote early compatible pollen responses in the *Arabidopsis thaliana* pistil. *Journal of Experimental Botany* **72**: 1198–1211.

Lenth R, Singmann H, Love J, Buerkner P, Herve M. 2019. *R Package emmeans*. CRAN. [WWW Document] URL https://CRAN.R-project.org/package=emmeans [accessed 15 June 2023].

Li D, Baldwin IT, Gaquerel E. 2015. Navigating natural variation in herbivory-induced secondary metabolism in coyote tobacco populations using MS/MS structural analysis. *Proceedings of the National Academy of Sciences, USA* **112**: 4147–4155.

Li W, Chetelat RT. 2015. Unilateral incompatibility gene *ui1.1* encodes an S-locus F-box protein expressed in pollen of *Solanum* species. *Proceedings of the National Academy of Sciences, USA* **112**: 4417–4422.

Mašková T, Herben T. 2018. Root : shoot ratio in developing seedlings: how seedlings change their allocation in response to seed mass and ambient nutrient supply. *Ecology and Evolution* **8**: 7143–7150.

McClure BA, Gray JE, Anderson MA, Clarke AE. 1990. Self-incompatibility in *Nicotiana alata* involves degradation of pollen rRNA. *Nature* **347**: 757–760.

Muñoz-Sanz JV, Zuriaga E, Cruz-García F, McClure B, Romero C. 2020. Self-(in)compatibility systems: target traits for crop production, plant breeding, and biotechnology. *Frontiers in Plant Science* **11**: 195.

Pannell JR, Voillemot M. 2017. Evolution and ecology of plant mating systems. In: *Encyclopedia of life sciences*. Chichester, UK: John Wiley & Sons, 1–9.

R Core Team. 2020. *R: a language and environment for statistical computing*. Vienna, Austria: R Foundation for Statistical Computing.

R Studio Team. 2020. *RSTUDIO: integrated development for R*. Boston, MA, USA: RStudio, PBC.

Raunsgard A, Opedal ØH, Ekrem RK, Wright J, Bolstad GH, Armbruster WS, Pélabon C. 2018. Intersexual conflict over seed size is stronger in more outcrossed populations of a mixed-mating plant. *Proceedings of the National Academy of Sciences, USA* **115**: 11561–11566.

Raxwal VK, Riha K. 2023. The biological functions of nonsense-mediated mRNA decay in plants: RNA quality control and beyond. *Biochemical Society Transactions* **51**: 31–39.

Raxwal VK, Simpson CG, Gloggnitzer J, Entinze JC, Guo W, Zhang R, Brown JWS, Riha K. 2020. Nonsense-mediated RNA decay factor UPF1 is critical for posttranscriptional and translational gene regulation in *Arabidopsis*. *Plant Cell* **32**: 2725–2741.

Ray R, Halitschke R, Gase K, Leddy SM, Schuman MC, Rodde N, Baldwin IT. 2023. A persistent major mutation in canonical jasmonate signaling is embedded in an herbivory-elicited gene network. *Proceedings of the National Academy of Sciences, USA* **120**: e2308500120.

Schuman MC, Heinzel N, Gaquerel E, Svatos A, Baldwin IT. 2009. Polymorphism in jasmonate signaling partially accounts for the variety of volatiles produced by *Nicotiana attenuata* plants in a native population. *New Phytologist* **183**: 1134–1148.

Sime KR, Baldwin IT. 2003. Opportunistic out-crossing in *Nicotiana attenuata* (Solanaceae), a predominantly self-fertilizing native tobacco. *BMC Ecology* **3**: 6.

Smith CC, Fretwell SD. 1974. The optimal balance between size and number of offspring. *The American Naturalist* **108**: 499–506.

Sun L, Williams JS, Li S, Wu L, Khatri WA, Stone PG, Keebaugh MD, Kao TH. 2018. S-locus F-box proteins are solely responsible for S-RNase-based self-incompatibility of *Petunia* pollen. *Plant Cell* **30**: 2959–2972.

Takayama S, Isogai A. 2005. Self-incompatibility in plants. *Annual Review of Plant Biology* **56**: 467–489.

Therneau TM. 2022. *A package for survival analysis in R*. R Package v.3.3.-1. [WWW document] URL https://cran.r-project.org/web/packages/survival/index.html [accessed 15 June 2023].

Tumpa K, Vidaković A, Drvodelić D, Šango M, Idžojtić M, Perković I, Poljak I. 2021. The effect of seed size on germination and seedling growth in sweet chestnut (*Castanea sativa* Mill.). *Forests* **12**: 858.

Van Daele I, Gonzalez N, Vercauteren I, de Smet L, Inzé D, Roldán-Ruiz I, Vuylsteke M. 2012. A comparative study of seed yield parameters in *Arabidopsis thaliana* mutants and transgenics. *Plant Biotechnology Journal* **10**: 488–500.

Wang J, Zhang Z. 2021. GAPIT version 3: boosting power and accuracy for genomic association and prediction. *Genomics, Proteomics & Bioinformatics* **19**: 629–640.

Whitehead MR, Lanfear R, Mitchell RJ, Karron JD. 2018. Plant mating systems often vary widely among populations. *Frontiers in Ecology and Evolution* **6**: 38.

Yoine M, Nishii T, Nakamura K. 2006. Arabidopsis UPF1 RNA helicase for nonsense-mediated mRNA decay is involved in seed size control and is essential for growth. *Plant & Cell Physiology* **47**: 572–580.

Zacchello G, Vinyeta M, Agren J. 2020. Strong stabilizing selection on timing of germination in a Mediterranean population of *Arabidopsis thaliana*. *American Journal of Botany* **107**: 1518–1526.

Zuur A, Ieno EN, Walker N, Saveliev AA, Smith GM. 2009. *Mixed effects models and extensions in ecology with R*. New York, NY, USA: Springer.

Supporting Information

Additional Supporting Information may be found online in the Supporting Information section at the end of the article.

Fig. S1 Quantification of the postpollination ethylene burst in 650 recombinant inbred lines from a 26-parent Multiparent Advanced Generation Inter-Cross population of *Nicotiana attenuata*.

Fig. S2 Manhattan plots summarizing the results of the Genome-Wide Association Study on the postpollination ethylene burst in *Nicotiana attenuata*.

Fig. S3 Variation in *Nicotiana attenuata* seedling phenotype.

Fig. S4 Early growth dynamics of *Nicotiana attenuata* seedlings of different parental genotype combinations.

Fig. S5 Germination time and number of leaves and secondary roots of *Nicotiana attenuata* seedlings 14 d after sowing.

Table S1 List of primers used in this study.

Table S2 Spearman's rank correlation coefficients between PPEB and the gene expression and protein abundance of SLR1 and SLR2 in *Nicotiana attenuata*.

Table S3 Genome-Wide Association Study results for the SNPs associated with the postpollination ethylene burst in the *Nicotiana attenuata* 26-parent Multiparent Advanced Generation Inter-Cross population after pollination with Utah wild-type standard pollen donor.

Table S4 Genes selected as candidates for further research after the Genome-Wide Association Study on postpollination ethylene burst in *Nicotiana attenuata*.

Please note: Wiley is not responsible for the content or functionality of any Supporting Information supplied by the authors. Any queries (other than missing material) should be directed to the *New Phytologist* Central Office.